Circuit influence on Cooper-pair current in solid-state entanglers

Vladimir Bubanja[1] and Shuichi Iwabuchi[2]
[1]*Industrial Research Ltd., P.O. Box 31-310, Lower Hutt 5040, Wellington, New Zealand*
[2]*Department of Physics, Graduate School for Interdisciplinary Scientific Phenomena and Information, Nara Women's University, Kitauoya-Nishimachi, Nara 630-8506, Japan*

(Received 4 April 2011; revised manuscript received 8 July 2011; published 6 September 2011)

We study the effects of the circuit impedance on tunneling of Cooper pairs from a superconductor into two normal-metal leads. We derive the expressions for the crossed and direct Andreev current and consider the limits of ballistic and diffusive electron motion in the electrodes. The derived analytic expressions show that voltage cross correlations, induced by the capacitive coupling of normal-metal leads, narrow the region where the crossed Andreev current dominates over the direct Andreev current, thereby reducing the efficiency of the entangler.

DOI: 10.1103/PhysRevB.84.094501 PACS number(s): 03.67.Bg, 73.23.Hk, 74.45.+c

I. INTRODUCTION

Hybrid nanostructured devices, consisting of a superconductor that is tunnel coupled to a normal metal, a semiconductor, or a topological insulator, have received considerable attention recently due to the rich novel physics involved as well as possible applications. They have been investigated as possible detectors of Majorana fermions,[1,2] detectors of magnetization switching of single magnetic molecules,[3] nanomechanical resonators,[4] accurate current sources,[5] as well as generators of mobile Einstein-Podolsky-Rosen (EPR) pairs.[6–8] The interesting new phenomena in these devices result from the interplay between the electronic states on each side of the interface between the two materials. In particular, in the case of the superconductor–normal-metal interface at subgap conditions, that is, at low temperatures and applied voltages compared to the superconducting energy gap, the relevant transport mechanism is Andreev reflection.[9,10] In this process, an electron incident from the normal-metal side is retroreflected as a hole with the creation of a Cooper pair on the superconductor side. If two normal-metal leads are connected to a superconductor via tunnel junctions separated by a distance that is of the order of the superconducting coherence length, the Cooper pair can split in a process termed "crossed Andreev reflection,"[7,8,11–16] producing two electrons that are separated in orbital space and entangled in spin space. Such EPR pairs are natural candidates for the solid-state implementation of quantum key distribution protocols due to weak coupling of the spin degrees of freedom to the environment, resulting in long coherence lengths and decoherence times.[17,18] Due to difficulties associated with the decoherence of electrons in the solid state, before the advent of nanofabrication tools, the original experiments with EPR pairs were done with polarization-entangled photons, including demonstration of the violation of Bell's inequalities.[19] This has not yet been done with electrons. On the other hand, experiments with electrons have an advantage over those with photons because the coincidence rate can be achieved without the need to synchronize the arrival times. This has enabled the recent demonstration of orbital entanglement in a fermionic Hanbury-Brown–Twiss two-particle interferometer using cross-correlation measurements.[20] Besides the fundamental importance of verifying Bell's inequalities in solid-state systems, electronic EPR pairs offer possibilities for future technologies based on quantum cryptography,[21] teleportation,[22,23] and information processing,[24] all of which could be integrated with existing electronics.

For the fabrication of more elaborate devices, as well as large-scale integration purposes, it is essential to consider the effects of the circuit layout on the Cooper-pair splitting process. In this paper we consider a solid-state entangler, schematically represented in Fig. 1. We include linear impedances at each branch of the three-port device, as well as the cross capacitance between the normal-metal leads. For close spacing between the leads, this stray capacitance cannot be neglected, since it gives rise to correlations between voltage fluctuations on different junctions. We find that these cross correlations reduce the efficiency of the entangler.

II. METHOD AND RESULTS

The Hamiltonian of our system is given by

$$H = H_0 + H_T, \tag{1}$$

where the unperturbed part,

$$H_0 = H_S + H_L + H_{\mathrm{EM}}, \tag{2}$$

$$H_S = \sum_{\mathbf{k},\sigma} E_{\mathbf{k}} \gamma^\dagger_{\mathbf{k},\sigma}\gamma_{\mathbf{k},\sigma}, \quad H_L = \sum_{i=1,2;\mathbf{k},\sigma} \epsilon^{(i)}_{\mathbf{k}} c^{(i)\dagger}_{\mathbf{k},\sigma} c^{(i)}_{\mathbf{k},\sigma}, \tag{3}$$

$$H_{\mathrm{EM}} = \sum_{\mathbf{q}} \hbar\omega(\mathbf{q})\, b^\dagger_{\mathbf{q}} b_{\mathbf{q}}, \tag{4}$$

consists of the terms describing the superconductor H_S (with quasiparticle operators describing the excitations out of the BCS ground state related to electron annihilation and creation operators via the Bogoliubov transformations, i.e., $c_{\mathbf{k},\sigma} = u_{\mathbf{k}}\gamma_{\mathbf{k},\sigma} + \sigma v_{\mathbf{k}}\gamma^\dagger_{-\mathbf{k},-\sigma}$, $u^2_{\mathbf{k}} = 1 - v^2_{\mathbf{k}} = (1 + \xi_{\mathbf{k}}/E_{\mathbf{k}})/2$, $E_{\mathbf{k}} = (\xi^2_{\mathbf{k}} + \Delta^2)^{1/2}$), normal-metal leads H_L, and the electromagnetic environment H_{EM}. This last term describes the three Ohmic circuit elements and a cross capacitance between the leads, corresponding to the circuit schematically represented in Fig. 1. The tunneling term is treated as a

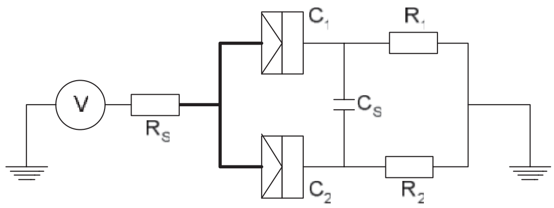

FIG. 1. Electrical circuit diagram of the system studied; the solid lines indicate the superconductor.

perturbation, and is given by

$$H_T = \sum_{i=1,2} H_i, \quad H_i = H_i^+ + H_i^-, \quad H_i^- = (H_i^+)^\dagger,$$
$$H_i^+ = \sum_\sigma \int d\mathbf{r}_1 d\mathbf{r}_2 T^{(i)}(\mathbf{r}_1,\mathbf{r}_2)\psi_\sigma^{(i)\dagger}(\mathbf{r}_1)\Psi_\sigma(\mathbf{r}_2)e^{-i\phi_i}, \tag{5}$$

where the field operators for the normal leads $\psi_\sigma^{(i)}(\mathbf{r})$ and the superconductor $\Psi_\sigma(\mathbf{r})$ are given by

$$\psi_\sigma^{(i)}(\mathbf{r}) = \frac{1}{\sqrt{V^{(i)}}}\sum_{\mathbf{k}} c_{\mathbf{k},\sigma}^{(i)} e^{i\mathbf{k}\cdot\mathbf{r}}, \tag{6}$$

$$\Psi_\sigma(\mathbf{r}) = \frac{1}{\sqrt{V^{(S)}}}\sum_{\mathbf{k}} c_{\mathbf{k},\sigma} e^{i\mathbf{k}\cdot\mathbf{r}}, \tag{7}$$

and the phase ϕ_i consists of the classical and quantum parts

$$\phi_i = \frac{e}{\hbar}Vt + \tilde{\phi}_i. \tag{8}$$

In the transition matrix approach,[12] the current consisting of Cooper pairs is given by

$$I = \frac{4\pi e}{\hbar}\sum_{f,i}|\langle f|T(\epsilon_i + i\eta)|i\rangle|^2\rho_i\delta(\epsilon_f - \epsilon_i), \tag{9}$$

where $\eta \to 0^+$, and the transition matrix is given by

$$T(\epsilon) = H_T\sum_{n=0}^{\infty}\left(\frac{1}{\epsilon - H_0}H_T\right)^n, \tag{10}$$

and $\rho_i = \langle i|\rho|i\rangle$ is the stationary occupation probability of the initial state $|i\rangle$. The current in the above expression (9), $I = I_{\rm CA} + I_{\rm DA}$, consists of the crossed Andreev current (where electrons from a Cooper pair tunnel into different leads), and the direct Andreev current (both electrons tunnel into the same lead). The lowest-order contribution to the current comes from Cooper-pair tunneling, since we consider low temperatures, $k_BT \ll \Delta$, and therefore assuming that there are no quasiparticles on the superconductor. The crossed Andreev term is given by

$$I_{\rm CA} = \frac{2e}{\hbar^4}\int_{-\infty}^{\infty}dt\int_0^{\infty}dt'\int_0^{\infty}dt'' e^{-\eta(t'+t'')} \times \sum_{\substack{i\neq i',\\ j\neq j',}}\langle H_j^-(t-t'')H_{j'}^-(t)H_i^+(t')H_{i'}^+(0)\rangle, \tag{11}$$

where the tunnel Hamiltonian terms are expressed in the interaction picture, and the expectation value is taken with respect to the density matrix of the unperturbed system. By substituting (5) into (11), we obtain

$$\begin{aligned}&\langle H_j^-(t-t'')H_{j'}^-(t)H_i^+(t')H_{i'}^+(0)\rangle\\ &= \sum_\sigma\int d\mathbf{r}_1,\ldots,d\mathbf{r}_8 T^{(j)*}(\mathbf{r}_1,\mathbf{r}_2)T^{(j')*}(\mathbf{r}_3,\mathbf{r}_4)T^{(i)}(\mathbf{r}_5,\mathbf{r}_6)\\ &\quad\times T^{(i')}(\mathbf{r}_7,\mathbf{r}_8)\big[-\mathcal{F}_\sigma^*(\mathbf{r}_4,\mathbf{r}_2,t'')\mathcal{F}_{-\sigma}(\mathbf{r}_6,\mathbf{r}_8,t')\\ &\quad\times\mathcal{G}_\sigma^{(i)>}(\mathbf{r}_1,\mathbf{r}_5,t-t'-t'')\mathcal{G}_{-\sigma}^{(i')>}(\mathbf{r}_3,\mathbf{r}_7,t)\delta_{i,j}\delta_{i',j'}\\ &\quad+\mathcal{F}_\sigma^*(\mathbf{r}_4,\mathbf{r}_2,t'')\mathcal{F}_\sigma(\mathbf{r}_6,\mathbf{r}_8,t')\mathcal{G}_\sigma^{(j)>}(\mathbf{r}_1,\mathbf{r}_7,t-t'')\\ &\quad\times\mathcal{G}_{-\sigma}^{(i)>}(\mathbf{r}_3,\mathbf{r}_5,t-t')\delta_{i',j}\delta_{i,j'}\big]\langle e^{i\phi_j(t-t'')}e^{i\phi_{j'}(t)}e^{-i\phi_i(t')}e^{-i\phi_{i'}(0)}\rangle,\end{aligned} \tag{12}$$

where the Green's functions in the leads, $\mathcal{G}_\sigma^{(i)>}(\mathbf{r},\mathbf{r}',t)$, and the anomalous Green's function in the superconductor, $\mathcal{F}_\sigma(\mathbf{r},\mathbf{r}',t)$, are introduced as

$$\mathcal{G}_\sigma^{(i)>}(\mathbf{r},\mathbf{r}',t) = \big\langle\psi_\sigma^{(i)}(\mathbf{r},t)\psi_\sigma^{(i)\dagger}(\mathbf{r}',0)\big\rangle, \tag{13}$$

$$\mathcal{F}_\sigma(\mathbf{r},\mathbf{r}',t) = \langle\Psi_{-\sigma}(\mathbf{r},t)\Psi_\sigma(\mathbf{r}',0)\rangle. \tag{14}$$

By assuming that the junctions are point-contact-like (i.e., their linear dimension is much larger than the Fermi wavelength, and much smaller than the superconducting coherence length; with the separation between junctions being much larger than the linear dimension of the junctions) and the tunnel matrix element $T^{(i)}(\mathbf{r}_1,\mathbf{r}_2)$ is nonzero only near the junction i, that is,

$$T^{(i)}(\mathbf{r}_1,\mathbf{r}_2) \sim t_0^{(i)}\delta(\mathbf{r}_1 - \mathbf{r}^{(i)})\delta(\mathbf{r}_2 - \mathbf{r}^{(i)}), \tag{15}$$

where $t_0^{(i)} = T^{(i)}\sqrt{V^{(i)}V^{(S)}}$, we can write

$$\begin{aligned}&\sum_{\substack{i\neq i'\\ j\neq j'}}\langle H_j^-(t-t'')H_{j'}^-(t)H_i^+(t')H_{i'}^+(0)\rangle\\ &= \sum_{i\neq j,\sigma}\big|t_0^{(i)}\big|^2\big|t_0^{(j)}\big|^2\big[\mathcal{G}_\sigma^{(j)>}(t-t'')\mathcal{G}_{-\sigma}^{(i)>}(t-t')\mathcal{F}_\sigma(\mathbf{r}^{(i)},\mathbf{r}^{(j)},t')\\ &\quad\times\mathcal{F}_\sigma^*(\mathbf{r}^{(i)},\mathbf{r}^{(j)},t'')\langle e^{i\phi_j(t-t'')}e^{i\phi_i(t)}e^{-i\phi_i(t')}e^{-i\phi_j(0)}\rangle\\ &\quad-\mathcal{G}_{-\sigma}^{(i)>}(t-t'-t'')\mathcal{G}_\sigma^{(j)>}(t)\mathcal{F}_\sigma(\mathbf{r}^{(i)},\mathbf{r}^{(j)},t')\mathcal{F}_{-\sigma}^*(\mathbf{r}^{(j)},\mathbf{r}^{(i)},t'')\\ &\quad\times\langle e^{i\phi_i(t-t'')}e^{i\phi_j(t)}e^{-i\phi_i(t')}e^{-i\phi_j(0)}\rangle\big],\end{aligned} \tag{16}$$

where

$$\mathcal{G}_\sigma^{(i)>}(t) = \langle\psi_\sigma^{(i)}(\mathbf{r}^{(i)},t)\psi_\sigma^{(i)\dagger}(\mathbf{r}^{(i)},0)\rangle = -i\frac{\nu^{(i)}\pi}{2\beta\sinh\left(\frac{\pi t}{\beta\hbar}\right)}, \tag{17}$$

$$\mathcal{F}_\sigma(\mathbf{r}^{(i)},\mathbf{r}^{(j)},t) = \frac{\sigma}{V^{(S)}}\sum_{\mathbf{k}}u_{\mathbf{k}}v_{\mathbf{k}}\big[e^{-iE_{\mathbf{k}}t/\hbar + i\mathbf{k}\cdot\delta\mathbf{r}_{ij}} - 2f(E_{\mathbf{k}})\cos(E_{\mathbf{k}}t/\hbar)e^{i\mathbf{k}\cdot\delta\mathbf{r}_{ij}}\big],$$

where $\nu^{(i)}$ is the density of states per volume of the lead i at the Fermi level, $\beta = 1/k_BT$, $\delta\mathbf{r}_{ij} = \mathbf{r}^{(i)} - \mathbf{r}^{(j)}$, and $f(\epsilon)$ is the Fermi function. By substituting (16) into (11), we get

$$\begin{aligned}I_{\rm CA} = {}&\frac{2e\big|t_0^{(1)}\big|^2\big|t_0^{(2)}\big|^2}{\hbar^4}\sum_{i\neq j,\sigma}\int_{-\infty}^{\infty}dt\int_0^{\infty}dt'\int_0^{\infty}dt'' e^{ieV(2t-t'-t'')/\hbar}\\ &\times\big\{\mathcal{G}_\sigma^{(j)>}(t-t'')\mathcal{G}_{-\sigma}^{(i)>}(t-t')\mathcal{F}_\sigma(\mathbf{r}^{(i)},\mathbf{r}^{(j)},t')\mathcal{F}_\sigma^*(\mathbf{r}^{(i)},\mathbf{r}^{(j)},t'')\\ &\times\exp[-J_{ij}(-t'') + J_{ij}(t-t'-t'') + J_j(t-t'')\end{aligned}$$

$$+ J_i(t-t') + J_{ij}(t) - J_{ij}(t')] - \mathcal{G}^{(i)>}_{-\sigma}(t-t'-t'') \times \mathcal{G}^{(j)>}_{\sigma}(t)\mathcal{F}_\sigma(\mathbf{r}^{(i)},\mathbf{r}^{(j)},t')\mathcal{F}^*_{-\sigma}(\mathbf{r}^{(j)},\mathbf{r}^{(i)},t'')\exp[-J_{ij}(-t'') + J_i(t-t'-t'')+J_{ij}(t-t'')+J_{ij}(t-t')+J_j(t)-J_{ij}(t')]\Big\}, \quad (18)$$

where

$$J_{ij}(t) = \langle\, [\tilde{\phi}_i(t)-\tilde{\phi}_i(0)]\tilde{\phi}_j(0)\rangle = \frac{e^2}{2\pi\hbar}\int_{-\infty}^{+\infty}\frac{d\omega}{\omega}\Re[Z_{ij}(\omega)]\left\{\coth\left(\frac{\beta\hbar\omega}{2}\right) \times[\cos(\omega t)-1] - i\sin(\omega t)\right\}, \quad (19)$$

where $Z_{ij}(\omega)$ is the cross impedance of the circuit in the absence of electron tunneling. The expression for $J_i(t)$ is obtained from (19) by replacing $Z_{ij}(\omega)$ with the effective circuit impedance $Z_i(\omega)$ as seen from the tunnel element i.[25] These impedances are in turn obtained by performing the star-triangle transformation and using Kirchhoff's rules for the circuit in Fig. 1. Hence, one can derive the short time behavior of the phase-phase correlations $J_i(t) \sim -iE_c^{(i)}t/\hbar$ (for $\Omega_i t \ll 1$), and $J_{ij}(t) \sim -iE_c^{(ij)}t/\hbar$ (for $\Omega_{ij} t \ll 1$). The expressions for the charging energies and characteristic frequencies are given in the Appendix. This short time behavior of the correlation functions enables us to obtain the expression for the crossed Andreev current in the high-bias regime, $\mathrm{eV} \gg \hbar\max(\Omega_i,\Omega_{ij})$, and $\Delta \gg (\mathrm{eV}-\bar{E}_c) \gg \hbar\max(\Omega_i,\Omega_{ij})$, where $\bar{E}_c = (E_c^{(1)}+E_c^{(2)})/2 + E_c^{(12)}$,

$$I_{\mathrm{CA}} = \frac{e\pi}{\hbar}\Gamma^{(1)}\Gamma^{(2)}S^2\Theta(\mathrm{eV}-\bar{E}_c)(\mathrm{eV}-\bar{E}_c),$$
$$\Gamma^{(i)} = \pi\nu^{(i)}\nu^{(S)}\big|t_0^{(i)}\big|^2, \quad S = \frac{\sin(k_F\delta r_{12})}{k_F\delta r_{12}}e^{-\frac{\delta r_{12}}{\pi\xi_0}}, \quad (20)$$

where $\Gamma^{(i)}$ is the dimensionless tunnel conductance of the junction i (normalized by $e^2/\hbar$), and ξ_0 is the Cooper-pair coherence length. When both electrons tunnel into the same branch i, we get

$$I_{\mathrm{DA}}^{(i)} = \frac{e\pi}{\hbar}\Gamma^{(\mathrm{i})2}S^2\Theta\big(\mathrm{eV}-2E_c^{(i)}\big)\big(\mathrm{eV}-2E_c^{(i)}\big). \quad (21)$$

In the low-bias regime, $\mathrm{eV} \ll \Delta,\hbar\min(\Omega_i,\Omega_{ij})$, we can use the long time behavior of the phase-phase correlations, $J_k(t) \sim -2z_k[\ln(i\Omega_k t)+\gamma]$, $z_k = \bar{R}_k/R_K$, where $k=i$ for direct and $k=ij$ for cross correlations, and where $\gamma = 0.577$ is the Euler's constant, to obtain the following for the crossed Andreev current:

$$I_{\mathrm{CA}} = \frac{e^2\pi}{\hbar}V\Gamma^{(1)}\Gamma^{(2)}S_a^2e^{-2\gamma(z_1+z_2)} \times\frac{\Gamma^2(1+2z_{12})}{\Gamma[2(1+z_1+z_2+2z_{12})]}\frac{(2\mathrm{eV})^{2(z_1+z_2+2z_{12})}}{\Delta^{4z_{12}}(\hbar\Omega_1)^{2z_1}(\hbar\Omega_2)^{2z_2}},$$
$$S_a = \frac{\sin(k_F\delta r_{12})}{k_F\delta r_{12}}\frac{2^{\frac{1}{2}-z_{12}}}{\sqrt{\pi}\Gamma(1+z_{12})} \times\left(\frac{\delta r_{12}}{\pi\xi_0}\right)^{\frac{1}{2}+z_{12}}K_{-\frac{1}{2}-z_{12}}\left(\frac{\delta r_{12}}{\pi\xi_0}\right), \quad (22)$$

where $K_\nu(x)$ is the modified Bessel function of the second kind. When both electrons forming a Cooper pair tunnel into the same branch i, in the low-bias limit, $\mathrm{eV} \ll \Delta,\hbar\min(\Omega_i,\Omega_{ij})$, and assuming $\Delta \gg \hbar\Omega_i$, $E_c^{(i)} < \Delta$, using the long time behavior of $J_i(t)$, we get

$$I_{\mathrm{DA}}^{(i)} = \frac{e^2\pi}{\hbar}V\Gamma^{(\mathrm{i})2}\left(\frac{4\Delta}{\pi\sqrt{\Delta^2-E_c^{(i)2}}}\tan^{-1}\sqrt{\frac{\Delta+E_c^{(i)}}{\Delta-E_c^{(i)}}}\right)^2 \times\frac{e^{-8\gamma z_i}}{\Gamma(2+8z_i)}\left(\frac{2\mathrm{eV}}{\hbar\Omega_i}\right)^{8z_i}, \quad (23)$$

where we assumed that electrons tunnel from the same point in the superconductor, $\delta r_{12} = 0$. For $\Delta \ll \hbar\Omega_i$, we get

$$I_{\mathrm{DA}}^{(i)} = \frac{e^2\pi}{\hbar}V\Gamma^{(\mathrm{i})2}P(z_i)\frac{(2\mathrm{eV})^{8z_i}}{(\hbar\Omega_i)^{4z_i}(\Delta)^{4z_i}},$$
$$P(z_i) = \frac{e^{-4\gamma z_i}}{\pi\Gamma(2+8z_i)}\left[\frac{\Gamma(1+2z_i)\Gamma\left(\frac{1}{2}+z_i\right)}{\Gamma(1+z_i)}\right]^2. \quad (24)$$

The above results, given by Eqs. (20)–(24), reduce to those obtained in Ref. 7, in the limit $R_1 = R_2 \equiv R$, $C_1 = C_2 \equiv C$, and $R_S/R = C_S/C = 0$.

The above considerations of ballistic electron motion can be generalized to include the disorder effects by expanding the field operators, instead of in the plane waves as in (6) and (7), into the complete set $\{\chi_k(\mathbf{r})\}$ of one-electron wave functions that satisfy the associated Schrödinger equation with the random impurity potential. In this case we obtain the following for the crossed Andreev current [see Fig. 2(a)]:

$$I_{\mathrm{CA}} = \frac{4e}{\hbar^4}\sum_{i\neq j}\int d\zeta d\zeta' d\xi d\xi' \;\; \Xi(\zeta,\zeta';\xi,\xi') \times[1-f(\xi)][1-f(\xi')]\mathcal{D}(\zeta,\zeta';\xi,\xi'), \quad (25)$$

where the function $\Xi(\zeta,\zeta';\xi,\xi')$ contains the information on geometry-dependent propagation:[8,26]

$$\Xi(\zeta,\zeta';\xi,\xi') = \int d\mathbf{r}_1,\ldots,d\mathbf{r}_8 \;\; T^{(i)*}(\mathbf{r}_1,\mathbf{r}_2)T^{(i)}(\mathbf{r}_5,\mathbf{r}_6) \times T^{(j)*}(\mathbf{r}_3,\mathbf{r}_4)T^{(j)}(\mathbf{r}_7,\mathbf{r}_8)K^*_\zeta(\mathbf{r}_4,\mathbf{r}_2)K_{\zeta'}(\mathbf{r}_6,\mathbf{r}_8) \times L_\xi^{(i)}(\mathbf{r}_1,\mathbf{r}_5)L_{\xi'}^{(j)}(\mathbf{r}_3,\mathbf{r}_7), \quad (26)$$

where the spectral functions are given, in terms of the advanced and retarded Green's functions, by $K_\zeta(\mathbf{r}_4,\mathbf{r}_2) = (G_\zeta^A - G_\zeta^R)/2\pi i$. The function $\mathcal{D}(\zeta,\zeta';\xi,\xi')$ contains the information on the electromagnetic environment,

$$\mathcal{D}(\zeta,\zeta';\xi,\xi') = u(\zeta)v(\zeta)u(\zeta')v(\zeta')\int_{-\infty}^{+\infty}dt\int_0^\infty dt'\int_0^\infty dt'' e^{i(2\mathrm{eV}-\xi-\xi')t/\hbar} \times e^{i[-E(\zeta')+\xi-\mathrm{eV}]t'/\hbar}e^{-J_{ij}(-t'')-J_{ij}(t')}[e^{i[E(\zeta)+\xi-\mathrm{eV}]t''/\hbar} \times e^{J_i(t-t'-t'')+J_{ij}(t-t'')+J_{ij}(t-t')+J_j(t)} + e^{i[E(\zeta)+\xi'-\mathrm{eV}]t''/\hbar} \times e^{J_{ij}(t-t'-t'')+J_j(t-t'')+J_i(t-t')+J_{ij}(t)}]. \quad (27)$$

The impurity-averaged spectral functions in the normal-metal leads are short ranged, with maximum value attained for the coinciding arguments, $\overline{L_\xi^{(i)}(\mathbf{r},\mathbf{r})} = \nu^{(i)}/2$. We assume that tunneling is local, $\mathbf{r}_{2k-1} \approx \mathbf{r}_{2k}$ for $k = 1,\ldots,4$, and for the interference effect in the superconducting electrode to be pronounced, we require $\mathbf{r}_4 \approx \mathbf{r}_6, \mathbf{r}_2 \approx \mathbf{r}_8$. Averaging of the

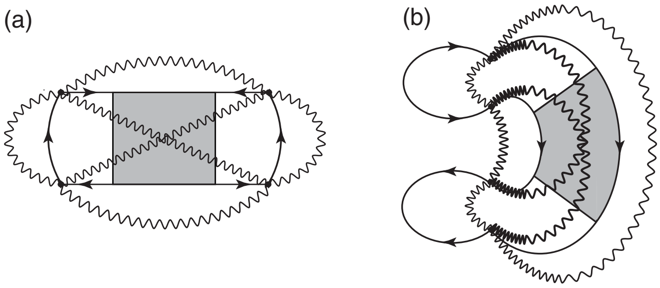

FIG. 2. Diagrams representing processes contributing to the subgap conductance. Double-arrowed lines represent anomalous propagators in the superconducting electrode, single-arrowed lines indicate the electron propagators in the normal-metal electrodes, and wiggly lines represent the phase correlators. Cooperon averaging over disorder (gray area) is performed (a) in the superconducting electrode, contributing to the crossed Andreev current, and (b) over disorder in the normal-metal electrode, contributing to the direct Andreev current.

spectral functions in the superconducting electrode produces a long-ranged function (with respect to Fermi wavelength),

$$\overline{K^*_\zeta(\mathbf{r},\mathbf{r}')K_{\zeta'}(\mathbf{r}',\mathbf{r})} = \frac{\nu^{(S)}}{4\pi}[\hat{\mathcal{P}}^{(S)}(\mathbf{r},\mathbf{r}',\zeta-\zeta') + \hat{\mathcal{P}}^{(S)}(\mathbf{r},\mathbf{r}',\zeta'-\zeta)], \quad (28)$$

where the Cooperon $\hat{\mathcal{P}}^{(S)}(\mathbf{r},\mathbf{r}',\zeta)$ satisfies the diffusion equation. After averaging, the function Ξ in (26) can be written as

$$\Xi = \frac{\hbar}{16\pi^3 e^4 \nu^{(S)}} \int_{S^{(1)}} d\mathbf{r} \int_{S^{(2)}} d\mathbf{r}' g^{(1)}(\mathbf{r}) g^{(2)}(\mathbf{r}') \times \int_{-\infty}^{+\infty} dt \; e^{i(\zeta-\zeta')t/\hbar} \mathcal{P}^{(S)}(\mathbf{r},\mathbf{r}',|t|), \quad (29)$$

where $g^{(i)}(\mathbf{r})$ is the conductance per unit area of the junction i, and the function $\mathcal{P}^{(S)}(\mathbf{r},\mathbf{r}',t)$, being the Fourier transform of $\hat{\mathcal{P}}^{(S)}$, describes the average probability that a particle evolves from $\mathbf{r}$ to $\mathbf{r}'$ in time t. For the environment of Fig. 1, at low voltages $\mathrm{eV} \ll \Delta$, we obtain the following for the function $\mathcal{D}$:

$$\mathcal{D} = \hbar^3\pi \frac{\Delta^2}{[E(\zeta)E(\zeta')]^{2(1+z_{ij})}} e^{-2\gamma(z_i+z_j)} \frac{\Gamma^2(1+2z_{ij})}{\Gamma[2(z_i+z_j+2z_{ij})]} \times \frac{(2\mathrm{eV}-\xi-\xi')^{2(z_i+z_j+2z_{ij})-1}}{(\hbar\Omega_i)^{2z_i}(\hbar\Omega_j)^{2z_j}} \Theta(2\mathrm{eV}-\xi-\xi'). \quad (30)$$

By substituting (29) and (30) into (25), we obtain

$$I_{\mathrm{CA}} = \frac{e^{-2\gamma(z_1+z_2)}}{e^3\nu^{(S)}} \frac{\Gamma^2(1+2z_{12})}{\Gamma[2(z_1+z_2+2z_{12}+1)]} \times \frac{(2\mathrm{eV})^{2(z_1+z_2+2z_{12})+1}}{(\hbar\Omega_1)^{2z_1}(\hbar\Omega_2)^{2z_2}\Delta^{4z_{12}}} \int_{S^{(1)}} d\mathbf{r} \int_{S^{(2)}} d\mathbf{r}' g^{(1)}(\mathbf{r}) g^{(2)}(\mathbf{r}') \times \int_0^\infty dt \; \mathcal{P}^{(S)}(\mathbf{r},\mathbf{r}',t)\mathcal{I}^2(t\Delta/\hbar),$$
$$\mathcal{I}(x) = \frac{2^{\frac{1}{2}-z_{12}}}{\sqrt{\pi}\Gamma(1+z_{12})} x^{\frac{1}{2}+z_{12}} K_{-1/2-z_{12}}(x). \quad (31)$$

For the large superconducting electrode, such that $L^2/D \gg \hbar/\Delta$, where L is the characteristic dimension of the electrode, we can use the probability for free diffusion in (31), which is in d dimensions given by $\mathcal{P}^{(S)} = e^{-|\mathbf{r}-\mathbf{r}'|^2/4Dt}/(4\pi Dt)^{d/2}$. In the absence of disorder, the probability is given by $\mathcal{P}^{(S)} = \delta(|\mathbf{r}-\mathbf{r}'|-\upsilon t)/A_d(|\mathbf{r}-\mathbf{r}'|)$, where υ is the group velocity and $A_d(R) = 2\pi^{d/2}R^{d-1}/\Gamma(d/2)$ is the surface area of the d-dimensional sphere. For $d=3$, we recover the expression (22), with the the sinusoidal term averaged over the Fermi wave vector directions. For the case of small-area junctions, and for $z_1 = z_2 \equiv z, \omega_1 = \omega_2 \equiv \omega_z$, and $z_{12} = 0$, we can write the crossed Andreev current as

$$I_{\mathrm{CA}} = \frac{e^2}{\hbar^2\nu^{(S)}} \frac{e^{-4\gamma z}\Gamma^{(1)}\Gamma^{(2)}V}{\Gamma(4z+2)} \left(\frac{2\mathrm{eV}}{\hbar\omega_z}\right)^{4z} \bar{\mathcal{P}}^{(S)}\left(|\mathbf{r}-\mathbf{r}'|, \frac{2\Delta}{\hbar}\right), \quad (32)$$

where $\bar{\mathcal{P}}^{(S)}$ is the Laplace transform of $\mathcal{P}^{(S)}$. Depending on the dimensionality, we have, in the diffusive regime, $\bar{\mathcal{P}}^{(S)}_{d=3} = e^{-\sqrt{2}\delta r/\xi^{(S)}}/4\pi D\delta r$, $\bar{\mathcal{P}}^{(S)}_{d=2} = K_0(\sqrt{2}\delta r/\xi^{(S)})/2\pi D$, and $\bar{\mathcal{P}}^{(S)}_{d=1} = e^{-\sqrt{2}\delta r/\xi^S}\xi^{(S)}/2\sqrt{2}D$, where $\xi^{(S)} = \sqrt{\hbar D/\Delta}$ (with D being the diffusion constant). In Ref. 27, the imbalance between the elastic cotunneling and crossed Andreev current observed in Ref. 14 was explained in terms of the spacial symmetry considerations of electromagnetic modes excited in the superconductor by the tunneling electron. The dominance of elastic cotunneling over the crossed Andreev current at low temperatures and voltages was observed by cross-correlation measurements in Ref. 28. We compare here the above result for the crossed Andreev current with the elastic cotunneling of Ref. 29. If we assume that the superconducting electrode is an island with charging energy $E_c^{(S)}$, and separate the corresponding pole from the impedance in the phase correlators in (27), we obtain that the cross Andreev current is vanishing for $\mathrm{eV} < 2E_c^{(S)}$, while no such blockade of tunneling exists for elastic cotunneling [formulas (15) and (16) in Ref. 29], and therefore elastic cotunneling is dominant at low voltages. By assuming that the characteristic diffusion time is short, so that the probability $\mathcal{P}^{(S)}$ is uniformly spread over the whole island, we obtain, from (32),

$$I_{\mathrm{CA}} = \frac{e^2\Gamma^{(1)}\Gamma^{(2)}\delta}{2\hbar\Gamma(4z+2)\Delta} e^{-4\gamma z} V \left(\frac{2\mathrm{eV}}{\hbar\omega_z}\right)^{4z}, \quad (33)$$

where δ denotes the average energy level spacing of the superconducting electrode. If instead of the voltage source connected to the superconducting electrode as in Fig. 1, voltage source V_i is connected to the normal-metal electrode i, we should replace V in (33) by $(V_1+V_2)/2$, and divide the expression by 2 in order to consider current in one branch only. This expression for the current then coincides with the elastic cotunneling in Ref. 29 (where one should replace V by $V_1 - V_2$, and further assume that $E_c^{(S)} \ll \Delta$).

The direct Andreev current into the lead i, $I_{\mathrm{DA}}^{(i)}$, is obtained from (25) by placing $j = i$ in (26) and (27). Apart from the diagram in Fig. 2(a), there are two more contributions corresponding to interference originating from the normal electrode, as well as interference occurring in both normal and superconducting electrodes. However, the phase of two electrons moving in the normal lead decays on the scale of $\xi^{(i)} = \sqrt{\hbar D/\mathrm{eV}}$, which at subgap conditions is much larger than the corresponding length in the superconducting electrode $\xi^{(S)}$. Therefore we only need to take into account the contribution of the diagram shown in Fig. 2(b). In the low-impedance limit $\mathrm{eV} \ll \Delta \ll \hbar\Omega_i$, we obtain the expression for $I_{\mathrm{DA}}^{(i)}$, which can be obtained from the above formula (31) by replacing $z_1 = z_2 = z_{12}$ by z_i, $g^{(1)} = g^{(2)}$ by $g^{(i)}$, $\nu^{(S)}$ by $\nu^{(i)}$, and $\mathcal{P}^{(S)}$ by $\mathcal{P}^{(i)}$. In the high-impedance limit $\mathrm{eV} \ll \hbar\Omega_i \ll \Delta$, we obtain

$$
\begin{aligned}
I_{\mathrm{DA}}^{(i)} &= \frac{4}{e^3\nu^{(i)}}\frac{e^{-8z_i\gamma}}{\Gamma(8z_i+2)}\frac{(2\mathrm{eV})^{8z_i+1}}{(\hbar\Omega_i)^{8z_i}}\int_{S^{(i)}} d\mathbf{r}d\mathbf{r}' g^{(i)}(\mathbf{r})g^{(i)}(\mathbf{r}')\\
&\quad\times\int_0^\infty dt\, \mathcal{Y}^2\big(t\Delta/\hbar, E_c^{(i)}/\Delta\big)\mathcal{P}^{(i)}(\mathbf{r},\mathbf{r}',t),\\
\mathcal{Y}(a,b) &= \frac{1}{\pi}\int_0^\infty dx \frac{\cos(xa)}{\sqrt{1+x^2}(\sqrt{1+x^2}-b)}.
\end{aligned}
\tag{34}
$$

For the case of point-contact tunnel junctions in the ballistic regime, Eq. (26) becomes $\Xi = \Gamma^{(i)2}/(4\pi)^2$, and after substituting in (31), we recover (23) and (24), in the high- and low-impedance cases, respectively.

III. CONCLUSION

We derive the expressions for the crossed and direct Andreev currents for an arbitrary electromagnetic environment, and consider the cases of ballistic and diffusive limits for electron motion. For the small superconducting electrode, the crossed Andreev current is blocked at low voltages and zero temperature, while in the elastic cotunneling case, the charging energy of the island only shifts the energy of the virtual state, without blocking the transport. At voltages above this gap and in the Ohmic environment, the two currents become equal functions of the relevant combination of voltage sources applied to the normal-metal electrodes ($V_1 + V_2$ for crossed Andreev current, and $V_1 - V_2$ for elastic cotunneling).

Equations (20) and (21) show that in the high-voltage regime, capacitive coupling reduces the voltage region, $\bar{E}_c < \mathrm{eV} < 2E_c^{(i)}$, where the crossed Andreev current dominates over the direct Andreev current. This is due to the appearance of the $E_c^{(12)}$ term in Eq. (20), which is directly proportional to the cross capacitance C_S. For the observation of entanglement in this limit, high-Ohmic leads, such as those successfully fabricated in metrology applications,[30,31] are essential to ensure Coulomb blockade.

It is of interest to consider the case of reflectionless tunneling, occurring for high transparency barriers due to disorder[32] or geometry.[33] In the present approach, that would require performing the summation to infinite order in (10), which is similar to the approach taken in Ref. 34.

ACKNOWLEDGMENTS

Fruitful discussions with S. V. Lotkhov and A. B. Zorin are gratefully acknowledged. We thank the Japan Society for the Promotion of Science for financial support.

APPENDIX

By performing the integration in (19), with $\Re[Z_i(\omega)] = (a_0 + a_2\omega^2)/(1 + b_2\omega^2 + b_4\omega^4)$, we obtain the short time behavior $\Omega_i t \ll 1$, of $J_i(t) \sim -iE_c^{(i)}t/\hbar$, where the charging energy is given by

$$
E_c^{(i)} = e^2(a_0\sqrt{b_4}+a_2)\frac{\sqrt{b_2+\sqrt{b_2^2-4b_4}}-\sqrt{b_2-\sqrt{b_2^2-4b_4}}}{2\sqrt{2b_4}\sqrt{b_2^2-4b_4}}. \tag{A1}
$$

The expressions for the coefficients, $a_0,\ldots,b_4$, are lengthy polynomials in the linear circuit elements of Fig. 1, and for the sake of brevity are not provided. However, they can be obtained straightforwardly from the total impedance seen from the tunnel junction i:

$$
\begin{aligned}
Z_i(\omega) &= \left[i\omega C_i + \frac{1}{Z_a(\omega)} + \frac{1}{Z_{\mathrm{eq}}(\omega)}\right]^{-1},\\
Z_a(\omega) &= \frac{\omega R_j(C_j + C_S) - i}{i\omega^2 C_j C_S R_j},
\end{aligned}
\tag{A2}
$$

$$
\begin{aligned}
Z_{\mathrm{eq}}(\omega) &= [1 + i\omega R_j(C_j + C_S)]\\
&\quad\times\left(\frac{R_S}{1 + i\omega[R_j(C_j + C_S) + R_S C_j]}\right.\\
&\quad\left.+\frac{R_i}{1 + i\omega[R_j(C_j + C_S) + R_i C_S]}\right).
\end{aligned}
$$

By substituting $\Re[Z_{ij}(\omega)]$ in (19), we obtain the short time behavior $\Omega_{ij}t \ll 1$, of $J_{ij}(t) \sim -iE_c^{(ij)}t/\hbar$, where the charging energy is given by

$$
E_c^{(ij)} = \frac{e^2}{(C_1C_2 + C_1C_S + C_2C_S)/C_S}. \tag{A3}
$$

The characteristic frequencies are given by

$$
\begin{aligned}
\Omega_i &= \frac{1}{\bar{R}_i\bar{C}_i}, \qquad \bar{R}_i = R_i + R_S,\\
\bar{C}_i &= 1/(R_i + R_S)^{3/2}\big[R_i^2(R_1 + R_2)C_S^2 - 2R_1R_2R_SC_2C_S\\
&\quad + (R_i + R_S)^3C_i^2 + R_S^2(R_j + R_S)C_j^2\\
&\quad + 2(R_i + R_S)(R_i^2C_S + R_S^2C_j)C_i\big]^{1/2},\\
\Omega_{ij} &= \frac{1}{\bar{R}_{ij}\bar{C}_{ij}}, \qquad \bar{R}_{ij} = R_S,\\
\bar{C}_{ij} &= \frac{1}{R_S^{3/2}}\big[C_1^2R_S(R_1 + R_S)^2 + C_2^2R_S(R_2 + R_S)^2\\
&\quad - C_S^2R_1R_2(R_1+R_2) - C_SC_1R_1(R_1R_2+R_2R_S - R_1R_S)\\
&\quad - C_SC_2R_2(R_1R_2 + R_1R_S - R_2R_S)\\
&\quad + C_1C_2R_S(R_1R_2 + R_1R_S + R_2R_S + 2R_S^2)\big]^{1/2}.
\end{aligned}
$$

[1] R. M. Lutchyn, J. D. Sau, and S. Das Sarma, Phys. Rev. Lett. **105**, 077001 (2010).
[2] Y. Oreg, G. Refael, and F. von Oppen, Phys. Rev. Lett. **105**, 177002 (2010).
[3] J.-P. Cleuziou, W. Wernsdorfer, V. Bouchiat, T. Ondarçuhu, and M. Monthioux, Nature Nanotech. **1**, 53 (2006).
[4] G. Sonne, M. E. Peña-Aza, L. Y. Gorelik, R. I. Shekhter, and M. Jonson, Phys. Rev. Lett. **104**, 226802 (2010).
[5] J. P. Pekola, J. J. Vartiainen, M. Möttönen, O.-P. Saira, M. Meschke, and D. V. Averin, Nature Phys. **4**, 120 (2008).
[6] L. G. Herrmann, F. Portier, P. Roche, A. Levy Yeyati, T. Kontos, and C. Strunk, Phys. Rev. Lett. **104**, 026801 (2010).
[7] P. Recher and D. Loss, Phys. Rev. Lett. **91**, 267003 (2003).
[8] G. Bignon, M. Houzet, F. Pistolesi, and F. W. J. Hekking, Europhys. Lett. **67**, 110 (2004).
[9] A. F. Andreev, Zh. Eksp. Teor. Fiz. **46**, 1823 (1964) [Sov. Phys. JETP **19**, 1228 (1964)].
[10] G. E. Blonder, M. Tinkham, and T. M. Klapwijk, Phys. Rev. B **25**, 4515 (1982).
[11] G. Falci, D. Feinberg, and F. J. W. Hekking, Europhys. Lett. **54**, 255 (2001).
[12] P. Recher and D. Loss, Phys. Rev. B **65**, 165327 (2002).
[13] D. Feinberg, Eur. Phys. J. B **36**, 419 (2003).
[14] S. Russo, M. Kroug, T. M. Klapwijk, and A. F. Morpurgo, Phys. Rev. Lett. **95**, 027002 (2005).
[15] L. Hofstetter, S. Csonka, J. Nygård, and C. Schönenberger, Nature (London) **461**, 960 (2009).
[16] D. Beckmann, H. B. Weber, and H. v. Löhneysen, Phys. Rev. Lett. **93**, 197003 (2004).
[17] J. R. Petta, A. C. Johnson, J. M. Taylor, E. A. Laird, A. Yacoby, M. D. Lukin, C. M. Marcus, M. P. Hanson, and A. C. Gossard, Science **309**, 2180 (2005).
[18] F. H. L. Koppens, J. A. Folk, J. M. Elzerman, R. Hanson, L. H. Willems van Beveren, I. T. Vink, H. P. Tranitz, W. Wegscheider, L. P. Kouwenhoven, and L. M. K. Vandersypen, Science **309**, 1346 (2005).
[19] A. Aspect, P. Grangier, and G. Roger, Phys. Rev. Lett. **49**, 91 (1982).
[20] I. Neder, N. Ofek, Y. Chung, M. Heiblum, D. Mahalu, and V. Umansky, Nature (London) **448**, 333 (2007).
[21] A. K. Ekert, Phys. Rev. Lett. **67**, 661 (1991).
[22] C. H. Bennett, G. Brassard, C. Crépeau, R. Jozsa, A. Peres, and W. K. Wootters, Phys. Rev. Lett. **70**, 1895 (1993).
[23] D. Bouwmeester, J.-W. Pan, K. Mattle, M. Eibl, H. Weinfurter, and A. Zeilinger, Nature (London) **390**, 575 (1997).
[24] M. A. Nielsen and I. L. Chuang, *Quantum Computation and Quantum Information* (Cambridge University Press, Cambridge, 2000).
[25] G.-L. Ingold and Yu. V. Nazarov, in *Single Charge Tunneling*, edited by H. Grabert and M. H. Devoret (Plenum, New York, 1992).
[26] F. W. J. Hekking and Yu. V. Nazarov, Phys. Rev. B **49**, 6847 (1994).
[27] A. Levy Yeyati, F. S. Bergeret, A. Martin-Rodero, and T. M. Klapwijk, Nature Phys. **3**, 455 (2007).
[28] J. Wei and V. Chandrasekhar, Nature Phys. **6**, 494 (2010).
[29] V. Bubanja, Phys. Rev. B **83**, 195312 (2011).
[30] A. B. Zorin, S. V. Lotkhov, H. Zangerle, and J. Niemeyer, J. Appl. Phys. **88**, 2665 (2000).
[31] S. V. Lotkhov, A. Kemppinen, S. Kafanov, J. P. Pekola, and A. B. Zorin, Appl. Phys. Lett. **95**, 112507 (2009).
[32] B. J. van Wees, P. de Vries, P. Magnée, and T. M. Klapwijk, Phys. Rev. Lett. **69**, 510 (1992).
[33] M. Schechter, Y. Imry, and Y. Levinson, Phys. Rev. B **64**, 224513 (2001).
[34] V. Bubanja and S. Iwabuchi, J. Phys. Soc. Jpn. **76**, 073601 (2007).